The transcription factor Pax6 is required for pancreatic β cell identity, glucose-regulated ATP synthesis and Ca2+ dynamics in adult mice

Mitchell, Ryan K.; Nguyen-Tu, Marie-Sophie; Chabosseau, Pauline; Callingham, Rebecca M.; Pullen, Timothy J; Cheung, Rebecca; Leclerc, Isabelle; Hodson, David J.; Rutter, Guy A.

DOI:
10.1074/jbc.M117.784629

The transcription factor *Pax6* is required for pancreatic β cell identity, glucose-regulated ATP synthesis and Ca^{2+} dynamics in adult mice

Ryan K. Mitchell[1], Marie-Sophie Nguyen-Tu[1], Pauline Chabosseau[1], Rebecca M. Callingham[1], Timothy J. Pullen[1], Rebecca Cheung[1], Isabelle Leclerc[1], David J. Hodson[1,2,3*], and Guy A. Rutter[1*]

[1]Section of Cell Biology and Functional Genomics, Division of Diabetes, Endocrinology and Metabolism, Imperial College London, Du Cane Road, London, W12 0NN, U.K.. [2]Institute of Metabolism and Systems Research (IMSR), and Centre of Membrane Proteins and Receptors (COMPARE), University of Birmingham, Edgbaston, B15 2TT, UK. [3]Centre for Endocrinology, Diabetes and Metabolism, Birmingham Health Partners, Birmingham, B15 2TH, UK.

Running Title**:** *Pax6 controls functional β cell identity*

*Correspondence to Professor Guy A. Rutter (g.rutter@imperial.ac.uk), Section of Cell Biology and Functional Genomics, Department of Medicine, Imperial College London, du Cane Road, London W12 0NN, U.K. Tel +44. 20.759.43340 or Dr David J. Hodson (d.hodson@imperial.ac.uk; d.hodson@bham.ac.uk) Institute of Metabolism and Systems Research (IMSR) and Centre of Membrane Proteins and Receptors (COMPARE), University of Birmingham, Edgbaston, B15 2TT, UK, Tel +44 (0) 121 414 6896

Key words: Insulin; diabetes; β cell; islet; Pax6; Ca^{2+}; connectivity; RNAseq

---

ABSTRACT

Heterozygous mutations in the human paired box gene *PAX6* lead to impaired glucose tolerance. Although embryonic deletion of the *Pax6* gene in mice leads to the loss of most pancreatic islet cell types, the functional consequences of *Pax6* loss in adults are poorly defined. Here, we developed a mouse line in which *Pax6* was selectively inactivated in β cells by crossing animals with floxed *Pax6* alleles to mice expressing the inducible Pdx1CreERT transgene. *Pax6* deficiency, achieved by tamoxifen injection, caused progressive hyperglycemia. While β-cell mass was preserved 8 days post injection, total insulin content and insulin:chromogranin A immunoreactivity were reduced by ~60%, and glucose-stimulated insulin secretion was eliminated. RNAseq and qRT-PCR analyses revealed that whereas the expression of key β cell genes including *Ins2*, *Slc30a8*, *MafA*, *Slc2a2*, *G6pc2* and *Glp1r* was reduced after *Pax6* deletion, that of several genes which are usually selectively repressed ("disallowed") in β-cells, including *Slc16a1*, was increased. Assessed in intact islets, glucose-induced ATP:ADP increases were significantly reduced ($p<0.05$) in β*Pax6*KO *versus* control β cells, and the former displayed attenuated increases in cytosolic Ca^{2+}. Unexpectedly, glucose-induced increases in intercellular connectivity were enhanced after *Pax6* deletion, consistent with increases in the expression of the glucose sensor glucokinase, but decreases in that of two transcription factors usually expressed in fully differentiated β-cells, *Pdx1* and *Nkx6.1*, as observed in islet "hub" cells. These results indicate that *Pax6* is required for the functional identity of adult β cells. Furthermore, deficiencies β cell glucose-sensing are likely to contribute to defective insulin secretion in human carriers of *PAX6* mutations.

INTRODUCTION

Defective insulin secretion underlies all forms of diabetes mellitus, a disease which now affects more than 422 m individuals worldwide (WHO: http://www.who.int/mediacentre/news/releases/2016/world-health-day/en/). Insulin is stored and released from β cells within pancreatic islets of Langerhans following elevations in glucose concentration (1). In response to high glucose, enhanced flux through glycolysis and mitochondrial oxidative metabolism (2) leads to increases in cytosolic ATP/ADP concentrations, the closure of ATP-sensitive K^+ (K_{ATP}) channels (3), cellular depolarisation and Ca^{2+} influx (4). Ca^{2+} sensors on secretory granules then catalyse hormone release through exocytosis (5). In the context of the intact islet, β cell-β cell connections (6,7) then create a coordinated network ensuring the optimal regulation of secretion through propagation of Ca^{2+} and other signals (8).

Paired box 6 (PAX6) is a transcription factor crucial for the development of the eye, brain, olfactory system and endocrine pancreas. Heterozygous mutations in the *PAX6* gene, which result in the production of a truncated, non-functional protein (9), cause abnormal iris formation (Aniridia) and impaired glucose tolerance (10). Correspondingly, PAX6 binding domains are found in the promoter regions of several key β cell genes (11), and islets derived from a human pedigree harbouring an inactivating missense *PAX6* mutation are deficient in proinsulin processing enzymes (PCSK1/3) (12). Interestingly, we observed no changes in *Pcsk1* expression in the present studies, arguing that the alterations observed in man may reflect an indirect action of PAX6. Furthermore, inheritance of the G allele at the single nucleotide polymorphism rs685428 lowers *PAX6* expression in man and is associated with increased fasting insulin and lower proinsulin:insulin ratio (13).

In mice, homozygocity for the 'small eye' *Pax6* mutant allele (Sey^{Neu}) leads to death at perinatal stages, and affected animals have dramatically reduced numbers of all islet cell types (14). Whilst deletion throughout the pancreas leads to overt diabetes and loss of β cells (15), heterozygous loss-of-function mutants show age- (12) and diet- (16) dependent impairments in glucose tolerance. Finally, *Pax6* expression is decreased in a rat model of T2D (the Zucker diabetic fatty rat; ZDF) (17)

Recent studies have also indicted that PAX6 may be important in maintaining the differentiated state and identity of the adult β cell. Thus, conditional inactivation of *Pax6* at post-natal stages in mice with a tamoxifen-inducible ubiquitous *Cre* leads to the development of a severe diabetic phenotype (18). Pancreatic analysis revealed a reduction in the expression of the *insulin* 1 and *insulin* 2, *glucagon* and *somatostatin* genes coupled with increases in the number of ghrelin-positive cells (18). The latter were also increased when deletion was restricted to either α or β cells in adult mice (19).

By contrast, few studies have examined how *Pax6* deletion affects the functional maturity of the adult β cell. One report (20), based on RNA interference, provided evidence that *Pax6* is required in the adult rat β cell for normal insulin secretion and the expression of key genes including *Ins1* and *Ins2*. However, the above approach was complicated by the requirement for β cell isolation prior to gene silencing, , and by potential off-target effects of silencing RNAs. Further, glucose sensing was examined in the latter study using isolated β cells rather than the intact islet, where responses to stimulation can differ markedly, and the gain of function resulting from inter-cellular interactions across the islet syncytium is lost (21). On the other hand, studies on the impact of *Pax6* deletion using *Cre*-mediated recombination in the adult have used either a ubiquitous *Cre* (18) or *Cre* expression driven by the rat insulin 2 promoter (RIP), which also leads to substantial recombination in the brain (22).

The aims of the present work were therefore: (i) to achieve efficient *Pax6* deletion selectively in the adult mouse β cell using targeted recombination at *flox*ed alleles with an alternative tamoxifen-inducible *Cre* system (Pdx1CreERT) (23,24); (ii) to examine β cell function and glucose-sensing *in vivo* and *in vitro* after *Pax6* ablation, and (iii) to determine the role of PAX6 in the control of a broader range of genes than has previously been examined, including those which are normally selectively silenced, or "disallowed", in mature β cells (25,26). Alongside decreases in the expression of β cell signature genes, up-regulation of the latter, which occurs in type 2 diabetes (27,28), is likely to report a loss of normal cellular identity.

We show that *Pax6* deletion achieved in this way leads to profound diabetes, consistent with earlier findings using alternative *Cre* drivers. Critically, we demonstrate marked abnormalities in gene expression, glucose metabolism, Ca^{2+} dynamics and insulin secretion in *βPax6*KO mouse islets early in the development of diabetes, which are likely to play an important part in β cell secretory failure. Unexpectedly, islets null for *Pax6* in the β cell display normal or enhanced cellular interconnectivity. Thus a functionally-interconnected β cell network can be maintained despite the partial loss of full β cell identity.

RESULTS

Efficient and inducible deletion of Pax6 *from the adult mouse β cell*

Mice harbouring *Lox*P sites surrounding exons 5, 5a and 6 of *Pax6* were crossed to Pdx1CreER mice. The breeding strategy used resulted in all animals carrying two copies of the floxed *Pax6* gene, but only half of these animals possessed a *Cre* allele (Cre^{+}; $Pax6^{fl/fl}$::Pdx1CreER$T^{+/-}$; β*Pax6*KO). Tamoxifen is expected to result in gene deletion only in animals that possess the *Cre* transgene (Figure 1A).

Eight week-old $Pax6^{fl/fl}$::Pdx1CreER$T^{+/-}$ and control $Pax6^{fl/fl}$::Pdx1CreER$T^{-/-}$ littermates were injected daily with tamoxifen (2 mg) for five days. Islets isolated two weeks after the final tamoxifen injection showed substantially (~70%) reduced levels of *Pax6* mRNA compared to littermate

controls (Figure 1B; 1.00 ± 0.00 *vs.* 0.35 ± 0.16 for *Cre*$^{-}$ vs. *Cre*$^{+}$; fold-change *vs. Cre*$^{-}$; p<0.01), consistent with deletion from the majority of the islet β cell compartment (~ 60 % of all cells) (29). A comparable reduction in PAX6 immunoreactivity was also observed by Western (immuno-) blotting (Figure 1C).

Immunocytochemical analysis of pancreatic slices for PAX6, insulin and glucagon assessed 8 days after the first tamoxifen injection (Figure 1D), revealed an ~80 % decrease in PAX6 staining across all islet cells (Fig. 1 D,E) with essentially complete (>98%) elimination of PAX6 immunoreactivity from β-cells and a more minor reduction (~25%) in α-cells (Fig. 1D,F), presumably reflecting maintained expression of *Pdx1* in a minority of α-cells, some of which may also express other islet hormones (30). We note that this *Cre* deleter strain does not catalyse significant recombination in the hypothalamus (31).

Despite a dramatic decrease in insulin immunoreactivity on a per cell basis (Figure 1D, g vs c) immunocytochemical analysis (Figure 1G), assessed at the same time point, revealed no significant changes in total β cell mass (Figure 1G; 0.23 ± 0.05 % *vs* control 0.17 ± 0.02 %; ns; Student's t test; *n*=4 animals per genotype), α cell mass (Figure 1H; 0.069 ± 0.019 % *vs* control 0.031 ± 0.004 %; ns; Student's t test; *n*=4) or β to α cell ratio (Fig. 1I; 4.3 ± 1.5 *vs* control 5.5 ± 0.9; ns; Student's t test; *n*=4).

Deletion of Pax6 *impairs glucose homeostasis* in vivo

β*Pax6* KO mice showed increased blood glucose levels from 8 days post final tamoxifen injection (Figure 2A; 9.45 ± 0.35 mM *vs.* 26.15 ± 1.13 mM for *Cre*$^{-}$ vs. *Cre*$^{+}$ respectively). This change was further exacerbated over time, with β*Pax6*KO animals showing an average glycaemia of 50.0 mM at the time of termination. Consistent with overt diabetes, the body weight of *βPax6*KO mice began to decline seven days after the final tamoxifen injection (Figure 2B). Two weeks post tamoxifen treatment, the decline in body weight was so severe that β*Pax6*KO mice were terminated in accordance with UK Home Office guidelines. We note that expression of the Pdx1CreERT transgene alone is not expected to impact insulin secretion or glucose tolerance (32). Correspondingly, *Pax6*$^{fl/fl}$::Pdx1CreERT$^{+/-}$ mice remained normoglycemic in the absence of tamoxifen administration (not shown). Likewise, tamoxifen alone, at the doses used here, exerts no effect on glycemia in wild-type C57BL/6J mice (31). Hence, any metabolic changes observed can reasonably be ascribed to the deletion of *Pax6*.

Insulin sensitivity, as assessed by intraperitoneal insulin tolerance test, was not markedly affected by *Pax6* deletion in β cells, despite increased blood glucose levels (Figure 2C). However, upon termination two weeks post tamoxifen treatment, blood glucose levels were significantly higher in β*Pax6*KO animals than littermate controls (Figure 2D; 9.10 ± 0.14 mM *vs.*47.2 ± 0.04 mM for *Cre*$^{-}$ *vs. Cre*$^{+}$; p<0.001). This change was accompanied by significantly decreased plasma insulin levels (Figure 2E; 1.51 ± 0.15 ng/mL vs 0.83 ± 0.16 ng/mL for *Cre*$^{-}$ vs. *Cre*$^{+}$; p<0.05) suggesting that the observed hyperglycaemia, caused by *Pax6* deletion, is likely to be due to insufficient insulin output from pancreatic β cells.

Total insulin levels, as measured in islets isolated from animals one week post tamoxifen treatment, were significantly reduced by *Pax6* deletion (Figure 2F; 14.5 ± 2.97 ng/mL/islet *vs.* 6.28 ± 1.57 ng/mL/islet for *Cre*$^{-}$ *vs. Cre*$^{+}$ respectively; p<0.05). A similar reduction, to levels observed after incubating at 3 mM glucose, was apparent after normalisation to islet DNA content (660 ± 63 *vs* 322 ± 69 ng insulin/ng DNA, p<0.05) or to total insulin content (0.41 ± 0.03 vs 0.016 ± 0.03 %, p <0.01). The latter observation excludes the possibility that our failure to detect an increase in insulin secretion from β*Pax6*KO islets after incubation at 17 *vs* 3 mM glucose simply reflects the lowered insulin content of KO *vs* control islets.

Finally, we measured basal and glucose-stimulated insulin secretion from isolated islets (Fig. 2G). Release of insulin from β*Pax6*KO islets tended to be lower than that from control islets when measured at 3 mM glucose but, in contrast to the ~4-fold stimulation observed in wild type islets at 17 mM glucose, no further increase was detectable from β*Pax6*KO islets at this higher glucose concentration (Fig. 2G). This altered response was not associated with any marked redistribution of granules away from the plasma membrane (i.e. in a reduction in the number of "morphologically-docked" granules), as assessed by TIRF microscopy (Fig. 2H,I), suggesting that defects later in granule release, or in the generation of metabolic signals required for exocytosis, are defective in this model.

Deletion of Pax6 *alters the expression of β cell signature and disallowed genes*

Consistent with a loss of β cell identity, the expression of *Ins2*, *Slc30a8*, *MafA*, *Slc2a2* and *Glp1r*, signature genes which are all highly expressed in healthy β cells and are essential for normal function (1), were all significantly reduced by *Pax6* deletion 8 days after tamoxifen treatment, as assessed by qRT-PCR analysis (Figure 3 A-E; p<0.05 *vs. Cre-* for all genes). In contrast, the

expression of the glucose sensor glucokinase (*Gck*) tended to increase (Figure 3F, ns *vs. Cre*$^-$). Interestingly, the expression of the β cell "disallowed" gene *Slc16a1,* encoding monocarboxylate transporter 1 (MCT-1), was significantly increased by *Pax6* deletion (Figure 3G, p<0.05 *vs. Cre*$^-$) at this stage. However, the expression of *Ldha*, another disallowed gene, was not affected (Figure 3H, p>0.05 *vs. Cre*$^-$).

As expected based on earlier models (18,19), glucagon expression was not significantly altered by *Pax6* deletion from β cells (Figure 3J, ns *vs. Cre*$^-$). Correspondingly, fasting plasma glucagon levels were also unchanged between control and *Pax6* null animals (147 ± 49.6 and 128 ± 28.7 pg/mL in control and β*Pax6*KO mice; *n*=4 and 6 animals respectively; p>0.05). In contrast, ghrelin expression was dramatically (>40 fold) increased (Figure 3K, p<0.05 *vs. Cre*$^-$).

To provide a transcriptome-wide assessment of the impact of *Pax6* deletion we next performed massive parallel RNA sequencing (RNAseq) on islets from control or null animals (Supplemental Figure S1). This revealed, firstly, that disallowed genes were selectively enriched amongst the up-regulated genes from β*Pax6*KO islets, as assessed by GSEA (Supplemental Figure S1A). Thus, of 58 members of the disallowed gene family included in the analysis (25), 38 were significantly enriched. These included both founder members of the group (*Slc16a1* and *Ldha*) (33) as well as the four other members (*Pdgfra, Cxcl12, Igfbp4* and *Oat*) of the shorter list of six genes common to (25,26) (Supplemental Figure S1B).

RNAseq also demonstrated that whereas markers of β cell progenitors, notably Neurogenin3, were up-regulated in response to the loss of PAX6, transcription factors characteristic of the fully differentiated β cell, including *Nkx6.1, Pdx1* and *MafA*, were repressed in knockout islets (Supplemental Figure S1C). Interestingly, these observations suggest that PAX6 may serve as either an activator or a repressor depending on context and target, as recently shown for the β cell enriched factors RFX6 (34) and Nkx2.2 (35).

The above approach also corroborated the changes observed above, including in the expression of *ghrelin* (increased 32-fold), *Ins2* (decreased 5.5-fold) and *Gck* (increased 2.8-fold) after *Pax6* deletion. *Gcg, Ppy, SSt,* expression were barely altered (Supplemental Figure S1D) and *Pcsk1 and Pcsk2* mRNA levels were essentially unchanged (Supplemental Figure S1E), arguing against alterations in prohormone processing. Affected genes included *Ero1lb,* a protein disulphide isomerise strongly enriched in β cells and likely involved in insulin maturation (36), and *G6pc2,* involved in glucose sensing (37), each being significantly down-regulated (Supplemental Figure S1E). Of note, we observed a large (156-fold; P=1.5x10^{-215}) increase in the expression of the voltage-gated potassium channel *Kcnj5*, likely to exert significant effects on membrane excitability and thus Ca^{2+} dynamics (Supplemental Figure S1E).

β*Pax6KO islet cells lose insulin expression but retain neuroendocrine properties*

Previous reports (19), and the above findings, indicate that *Pax6* null β cells are shunted towards an alternative cell fate. We therefore stained pancreatic slices obtained from animals eight days after the final tamoxifen injection for the neuroendocrine marker chromogranin A (38) alongside insulin and glucagon (Figure 4A). Expressing the number of total insulin and glucagon immunopositive area as a ratio of the total chromogranin A immunopositive area revealed that deletion of *Pax6* significantly reduced the insulin:chromogranin A ratio (Figure 4B; 0.89 ± 0.02 *vs*. 0.38 ± 0.02 for *Cre*$^-$ vs. *Cre*$^+$ respectively; p<0.001), while the glucagon:chromogranin A ratio was not significantly changed (Figure 4C; 0.14 ± 0.04 *vs*. 0.19 ± 0.02 for *Cre*$^-$ *vs*. *Cre*$^+$; ns).

Islets isolated from β*Pax6*KO *mice show impaired glucose-induced cytosolic ATP/ADP increases and intracellular* Ca^{2+} *dynamics*

Given the absence of glucose-stimulated insulin secretion, and changes in gene expression and apparent cellular identity observed above, we next determined whether disruption of *Pax6* may interfere with glucose metabolism or sensing by β cells within the intact islet. We used firstly the recombinant cytosol-targeted ATP/ADP probe, Perceval (39,40), and Nipkow spinning disc confocal microscopy (41,42). Expression of the above sensor is largely restricted to the β cell [34], due to the apparent tropism of adenoviruses towards this cell type (43). Exposure to high (11 mM) glucose caused a time-dependent increase in ATP/ADP ratio in control islets as expected (40,41), and this increase was reduced in amplitude by ~30% in β*Pax6*KO islets (Figure 5A, B; 0.15 ± 0.01 arbitrary units (AU)[1] vs. 0.11 ± 0.01 AU for *Cre*$^-$ vs. *Cre*$^+$ respectively; p<0.05, and Supplemental Movies 1 & 2). *Pax6* deletion also markedly reduced the number of glucose-responsive cells, as assessed at 11 mM glucose (Figure 5C & D; 53.9 ± 4.93 *vs.* 25.8 ± 2.30 for *Cre*$^-$ and *Cre*$^+$, respectively, p<0.001). Similar

[1] **Abbreviations**: AU, arbitrary units; GSEA, Gene Set Enrichment Analysis; K_{ATP}, ATP-sensitive K^+ channel

differences between β*Pax6* null and control islets were also apparent after stimulation at a lower glucose concentration (8 mM; Figure 5E,F; 0.07 ± 0.01 *vs* 0.02 ± 0.005 AU30 for *Cre*$^-$ and *Cre*$^+$, respectively, p<0.001)..

Since impairments in ATP generation are likely to affect the closure of K_{ATP} channels, impacting on plasma membrane depolarisation and Ca^{2+} influx (1), we next sought to determine how intracellular Ca^{2+} dynamics may be affected by *Pax6* deletion. Islets were therefore loaded with the trappable intracellular Ca^{2+} probe, fluo-2, and confocal imaging performed essentially as above (albeit at a higher acquisition rate). *Pax6* deletion reduced both the amplitude (Figure 6A; 0.90 ± 0.13 AU *vs*. 0.33 ± 0.04 AU for *Cre*$^-$ vs. *Cre*$^+$ respectively; p<0.001) and the area-under-the-curve (AUC; Figure 6A; 2819.8.1 ± 118.1 AU *vs*. 2248 ± 54.9 AU for *Cre*$^-$ *vs. Cre*$^+$; p<0.001) of glucose-evoked Ca^{2+} traces. Ca^{2+} responses to the depolarising stimulus KCl were unchanged by *Pax6* deletion (Figure 6B; Amplitude: 1.35 ± 0.13 AU *vs.*1.43 ± 0.12 AU for *Cre*$^-$ vs. *Cre*$^+$ respectively; AUC 1552 ± 60.2 vs. 1569 ± 61.1 for *Cre*$^-$ vs. *Cre*$^+$ respectively; both ns), suggesting that voltage-dependent Ca^{2+} channel function remains intact.

*Individual β cell Ca^{2+} responses in β*Pax6KO islets show high levels of coordination*

Although average islet Ca^{2+} responses to glucose were reduced by *Pax6* deletion (Figure 6A), the responses of individual β cells were also altered. Specifically, islet β cells derived from *Cre*$^-$ animals responded to glucose with a rapid and largely monophasic increase in free cytosolic Ca^{2+} that was synchronised across the islet (Figure 7A, top, and Supplemental Movie 3). By contrast, β*Pax6*KO β cells displayed a delayed and oscillatory response, although one which was well coordinated between individual β cells (Figure 7A, bottom, and Supplemental Movie 4). Subjecting individual β cell responses to analysis packages that map cell-cell coordination (8,44,45), it was possible to show that the percentage of cells that responded to glucose was unchanged by *Pax6* deletion (Figure 7B; 77.6 ± 5.39 % *vs*. 72.1 ± 4.81 % for *Cre*$^-$ vs. *Cre*$^+$ respectively; ns). However, the level of synchronicity between individual β cells tended to be higher in *βPax6*KO islets, as shown by an increase in the percentage of significantly correlated cell pairs (Figure 7C; 69.1 ± 7.40 % vs. 84.7 ± 3.79 % for *Cre*$^-$ vs. *Cre*$^+$ respectively; p=0.06). Furthermore, the strength of β cell connections was greater in *βPax6*KO islets, as shown by weighted graphs depicting location and strength of connections between individual cells (Figure 7D,E; 0.42 ± 0.09 R *vs.* 0.65 ± 0.04 R for *Cre*$^-$ *vs. Cre*$^+$ respectively; p<0.05). These changes were not associated with any alterations in the level of expression of the gap junction protein connexin 36, encoded by *Gjd2*, an important mediator of cell-cell interactions in the islet (7) (Figure 3I).

DISCUSSION

The present study sought to determine whether changes in cellular identity, previously described after *Pax6* inactivation in β cells (18,19), are accompanied by significant changes in β cell function, as well as the expression of key β cell genes involved in normal glucose sensing and insulin release. We also sought to determine the importance of *Pax6* in maintaining intercellular communication within the islet, a feature required for normal secretory responses to secretatogues and which becomes defective in type 2 diabetes (21).

The use here of the efficient and selective Pdx1CreERT driver line (23,24,31) led to the more rapid (within days of tamoxifen treatment) and severe (>50 mM) hyperglycaemia than previously observed after *Pax6* deletion either globally (18) or in β cells using the more promiscuous rat insulin promoter 2 (RIP2) Cre driver (19). Although limited recombination in the brain (chiefly in the basomedial hypothalamus) is also observed with Pdx1CreERT (22), deletion at extrapancreatic sites (19,22,46), or in islet non-β cells, may contribute to the milder phenotypes previously observed with earlier *Cre*s. Whilst recombination with Pdx1CreERT has previously been reported to be almost completely confined to β cells (24), we did detect a small degree of deletion of PAX6 in α cells. This difference with respect to earlier findings may reflect the differing susceptibility to *Cre* action of *Lox*P sites at different genomic locations (47). Of note, glucagon mRNA levels were not different between WT and KO mice (Fig. 3J Supplemental Figure S1D)). On the other hand, we observed a substantial increase in ghrelin expression (Fig. 3 K, Supplemental Figure S3D) after *Pax6* deletion which may reflect a cell fate switch of β (or possibly α) cells towards an ε cell phenotype, as previously proposed (19).

We consequently chose to study islets from β*Pax6*KO mice at relatively early time points after deletion to minimise the exposure *in vivo* to high glucose concentrations. This was felt important given earlier (48) and more recent (49) reports that hyperglycemia itself leads to a loss of β cell identity. Although at the time point post tamoxifen used in the present studies (8 days) a significant increase in fasting blood glucose was apparent (Figure 2), the alterations in insulin and glucagon expression observed after *Pax6* deletion were markedly different in both extent (insulin) and direction (glucagon) from those previously reported

in response to hyperglycemia induced by K_{ATP} channel activation in β cells (49). Moreover, in the present report, islets were cultured at near normal (11 mM) glucose for 24-48 hours after extraction, a manoeuvre expected to at least partially reverse any changes resulting from antecedent *in vivo* hyperglycemia. Finally, we observed no (qRT-PCR; Fig. 3H) or small (RNAseq; Supplemental Figure S1B) increases in *Ldha* expression, previously found to be reversibly up-regulated *in vivo* in islets by hyperglycemia (48). Thus, we conclude that alterations in gene expression and function observed in the present study are, at least in large part, a reflection of cell autonomous actions of *Pax6* rather than hyperglycemia *per se*. Notably, the expression of several key β cell genes was affected by *Pax6* ablation, with substantial decreases in *Ins2*, *Slc30a8 (ZnT8)*, *MafA*, *Slc2a2* (*Glut2*) and *Glp1r* mRNA levels (Figure 3). Whilst future work will be required to determine whether this reflects direct or indirect regulation of these genes by PAX6, we note that *Gck* gene expression was increased (Fig. 3F), demonstrating a degree of selectivity in the regulation of β cell-enriched genes by PAX6.

Interestingly, we also demonstrate that, after *Pax6* inactivation, a significant increase occurs in the expression of members of the β cell "disallowed" gene family, notably *Slc16a1*/MCT-1 (27). As far as we are aware, this is the first time that *Pax6* has been shown to regulate members of this group. Thus, PAX6 controls β cell identity both through driving the expression of essential glucose-sensing genes and by *repressing* a gene whose presence is deleterious to β cell function (50). In this respect, the actions of PAX6 resemble those of RFX6, shown recently to be necessary for both normal β cell development (51) and function (34).

Although, and in agreement with previous studies, total islet insulin content was reduced by *Pax6* deletion by ~60 % (Figure 2F), we were unable to detect any insulin secretion from *Pax6* null islets in response to glucose. Interestingly, and although explored in a relatively small number of animals (*n*=4/genotype), this was not associated with detectable decreases in overall β or α cell mass or in β/α cell ratio (Figure 1, G-I). Deploying cell-resolution imaging approaches, we demonstrate that this is associated with marked impairments in glucose-induced ATP/ADP increases, likely resulting from lowered Glut2 (*Slc2a2*), but not *Gck* expression (which was increased), and possibly increases in *Slc16a1*/MCT-1 levels, thus favouring anaerobic glycolysis. We also noted a substantial decrease in the expression of *G6pc2* (Figure 3N), likely to potentiate the effects of increased *Gck* expression and thus to increase net flux from glucose to glucose-6P. Since flux control at the initial stages of glycolysis is achieved chiefly at the glucokinase step (1), the above observations suggest that increased flow through the latter reaction is not met by a proportional increase at later stages of glycolysis or in the oxidation of pyruvate and NADH by mitochondria. Future studies will be needed to explore these possibilities in detail.

Of note, increased expression and release of ghrelin, and binding to ghrelin receptors which are enriched in delta cells (52) may also enhance somatostatin secretion to suppress insulin release.

Deletion of *Pax6* also drastically changed the profile of glucose-stimulated Ca^{2+} responses from an initial spike of Ca^{2+} activity followed by a sustained, oscillatory period (34,53) to more delayed and burst-like properties reminiscent of those observed in α cells (54). Interestingly, connectivity between cells was not significantly impaired by the loss of *Pax6*. Rather, we observed a tendency towards increased connectivity, and a significant increase in the strength of connections between cells (correlation coefficient; Figure 7D&E), despite unchanged *Gjd2* expression (Figure 3I). Thus, impaired β cell-β cell communication/connectivity does not drive altered glucose sensing in *Pax6* null β cells. Importantly, the present findings demonstrate that full β cell maturity is not a prerequisite for the formation of a functional interconnected network of cells. Indeed, we have recently shown the existence of a small population of immature β cells that express high levels of glucokinase and which dictate islet responses to glucose (55). Whether and how the activity of these putative "hub" or "pacemaker" cells within the islet is affected by *Pax6* deletion will be interesting to establish. Of note, elevated *Gck* expression, alongside substantially lower *Pdx1* and *Nkx6.1* expression, in β*Pax6*KO islets, are features characteristic of previously-described islet "hub" cells (55). These and other changes, including in ion channel expression (RNAseq; see Results and not shown), and glucose sensitivity, may thus contribute to the enhanced Ca^{2+} dynamics and connectivity observed after *Pax6* deletion.

Perhaps surprisingly, the partial defects in metabolic glucose signalling observed above (i.e. ATP/ADP and Ca^{2+} changes) were associated with an apparently complete loss of glucose-stimulated insulin secretion, assessed *in vitro*. This loss of insulin release was less marked *in vivo*, possibly reflecting alternative mechanisms for stimulating secretion in the living animal (e.g. actions of circulating amino acids or fatty acids, hormonal and neural inputs into the islet, etc) (1). Nevertheless, the results obtained with isolated islets would appear to indicate that PAX6 is also important in the β cell for K_{ATP} channel and Ca^{2+}-independent mechanisms of glucose-stimulated

insulin secretion (56). Whether enhanced β cell-β cell coupling can, in some settings, also be deleterious for the normal tight regulation of insulin secretion, is a possibility which also merits investigation.

Whilst the current study was under revision, a report (57) appeared using a similar approach but an alternative *Cre* (MIP.CreERT), based on the rat insulin 1 promoter, to delete *Pax6* in adult β cells. Importantly, Swisa et al (57) also identified, by Gene Ontology analysis, gene classes which may contribute to the enhanced connectivity observed in the present report, including ion channels and Ca^{2+} channels. As observed here, the phenotype of β *Pax6* null mice was remarkably severe, and was associated with ketosis and marked changes in secretory granule structure observed at the ultrastuctural level by electron microscopy. Thus, atypical granules, lacking a classical "halo" around the dense core, were frequently seen in null mouse islets. Importantly, lineage tracing work in the report by Swisa et al also demonstrated that "reprogammed" cells, expressing ghrelin, were derived from β cells. Finally, it was shown by ChIP-sequencing that PAX6 binds directly to sequences in target genes to affect their repression or activation. Importantly, however, the above study did not explore the regulation of insulin secretion or metabolic glucose signalling in *Pax6*-deleted β cells, as described in the present report.

As discussed above and elsewhere (58), use of the MIP.CreERT deleter strain may, however, be complicated by the concomitant over-expression of human growth hormone (hGH). Reassuringly, the strong similarities between the findings of our own study and those described in (57) indicate that the changes in each are chiefly attributable to altered *Pax6* expression.

EXPERIMENTAL PROCEDURES

Generation of βPax6KO mice

All animal procedures were approved by the Home Office according to the Animals (Scientific Procedures) Act 1986 of the United Kingdom (PPL 70/7349).

Mice homozygous for the *floxed* allele of *Pax6* (*Pax6*$^{fl/fl}$), kindly provided by Prof David Price, University of Edinburgh (59), were crossed to a tamoxifen-regulated deleter strain, provided by Dr Doug Melton (Harvard Medical School) in which *Cre* recombinase is expressed under the control of the Pdx1 promoter (Pdx1CreERT) (23). The breeding strategy ensured that 50% of the offspring inherited the *Cre* transgene (*Cre*$^{+}$, *βPax6*KO; Pdx1CreERT$^{+/-}$::Pax6$^{fl/fl}$), the remainder serving as littermate controls (*Cre*$^{-}$, Pdx1CreERT$^{-/-}$::Pax6$^{fl/fl}$). Gene deletion was achieved by five intraperitoneal tamoxifen injections (2 mg), administered daily to eight week old animals of both genotypes. Pdx1CreERT$^{+/-}$ mice displayed no evident metabolic abnormalities.

Insulin tolerance tests (ITT)

Bovine insulin (0.75 U/Kg body weight; Sigma, Dorset, UK) was injected into the abdomen of mice fasted for 5 hours. Blood glucose measurements were taken at time points 0, 15, 30 and 60 min. using an automatic glucometer (Accucheck).

Plasma Glucose & Insulin Measurements

Fed mice were culled and blood collected into EDTA coated tubes (Sarstedt, Beaumont Leys, UK). Glucose measurements were determined using an automatic glucometer (Accucheck). For insulin measurements, plasma was separated by centrifugation at 13,200 rpm. for 20 min, 5 µL of blood plasma was used to measure insulin levels using an ultrasensitive mouse insulin ELISA kit (CrystalChem, Netherlands). For total islet insulin measurements, five islets were lysed by sonication in acidified ethanol (1.5% HCl [vol./vol.], 75% ethanol [vol./vol.], 0. 1 % Triton X-100 [vol.vol]). Insulin concentration was determined using a HTRF-based assay kit (CisBio, USA).

Quantitative real time PCR (qRT-PCR)

RNA was extracted from isolated islets using Trizol reagent (Invitrogen, Paisley) and reverse transcribed using a high capacity reverse transcription kit (Invitrogen, Paisley). Relative gene expression was assessed using SYBR Green (Invitrogen, Paisley) and expression of each gene was normalized and expressed as n-fold change in mRNA expression versus Cre^{-}, calculated using the $2^{\wedge\Delta\Delta Ct}$ method (60).

Massive parallel sequencing of RNA (RNAseq)

Total RNA was extracted with Trizol from islets isolated from five knockout and four control mice. Polyadenylated transcripts were selected during the preparation of paired - end, directional RNA-Seq libraries. Libraries were sequenced on an Illumina HiSeq 2000 machine. The quality of the sequenced libraries was assessed using fastQC. Reads were mapped to the Grc38m assembly using HiSat2. Annotated transcripts were quantified using featureCounts and differentially expressed genes identified with DESeq2. All genes were ranked by fold-change and the resultant list used for gene set enrichment analysis. Gene Set Enrichment Analysis (GSEA) was performed essentially as described (61) and used the Broad Institute GSEA tool for analysis of pre-ranked lists http://software.broadinstitute.org/gsea/msigdb)

with a custom constructed geneset combining the disallowed genes identified in (25,26)

RNA-Seq accession codes

Raw sequence data for RNA-Seq will be made available via deposition to ArrayExpress (www.ebi.ac.uk/arrayexpress; Accession number xxxx).

Immunocytochemistry

Pancreata were extracted and fixed in 10% [vol./vol.] formalin, transferred into a tissue processing cassette and embedded in paraffin wax within 24 hours of being harvested from the mouse. Pancreatic sections were cut at 5 µm onto superfrost slides. Sections were dewaxed by immersing in histoclear (Sigma Aldrich, Dorset, UK) for 20 min before rehydration. Antigen retrieval was performed by boiling slides in citrate buffer (VectorLabs, Peterborough, UK), washed before blocking 3% [vol./vol.] goat/donkey serum (Dako, Cambridgshire, UK) in 2% BSA with 0.1% [vol./vol.] Triton-X100 for 1 h at room temperature. Slides were then washed before staining with primary antibody (guinea pig anti-insulin (1:200, DAKO), mouse anti-glucagon (1:1000, Sigma Aldrich), and rabbit anti-chromagranin A (1:200, Abcam). Slides were incubated in primary antibody overnight at 4 ^{0}C. Revelation was performed using a combination of the following secondary antibodies: donkey anti-rabbit 488, goat anti-guinea pig 643, goat anti-mouse 568 (all 1:500, Invitrogen, Paisley, UK). Slides were mounted using vectorshield mounting medium containing DAPI (Vectorlabs, Peterborough, UK) and a 24 mm coverslip placed over the slice. Slides were visualised by fluorescent microscopy using a Zeiss Axio Observer inverted widefield microscope with LED illumination running Zen acquisition software. Quantification of immunopositive area was achieved using ImageJ analysis software using a macro established in house. For quantification of β- and α-cell mass, slides were visualized using an Axiovert 200M microscope (Zeiss) with Alexa Fluor 488 goat anti-guinea pig IgG and with Alexa Fluor 568 goat anti-mouse IgG (Invitrogen) using an Axiovert 200 M microscope (Zeiss, Welwyn Garden City, UK) at the Facility for Imaging by Light Microscopy (FILM), Imperial College London.

In order to stain PAX6 an alternative protocol was used, based on a modification of the protocol described in (62). The main adaptions included permeabilisation with methanol [100%; -20°C] (3 min), more vigorous antigen retrieval via boiling in citrate-based antigen unmasking solution (Vector Laboratories; 15 min), enhanced blocking with 1% (w/v) skimmed milk (1.5 h), incubation with anti-glucagon antibody (1:500) alone 2.5 h before overnight incubation with remaining two primary antibodies (anti-PAX6 [Biolegend], 1:70; anti-insulin, 1:200) and a longer incubation with secondary antibody (2 h). Image acquisition was performed with a Zeiss Axio Observer inverted microscope fitted a Hamamatsu Flash4 camera. The filters used were: blue (365 nm LED; excitation 377/50; emission 477/60), green (470 nm LED; excitation 472/30; emission 520/35), red (540 - 580 nm LED; excitation 534/20; emission 572/28), and far red (625 nm LED; excitation 631/22; emission 688/20). Negative controls to assess non-specific binding were performed by omitting the incubation with primary antibodies.

Western (immuno-) blotting

Whole islet extracts were separated using a 10% acrylamide gel and blotted onto a polyvinylidene difluoride membrane. Following blocking for 60 min. with 5% (w/v) skimmed milk in TBST (10 mM Tris-base, pH 7.6, 150 mM NaCl, 0.1% Tween 20) membranes were incubated overnight at 4^{o}C with antibody an against Pax6 (1:300, Biolegend). The membrane was washed three times (5 min. each) with TBST before incubation of the secondary anti-rabbit HRP antibody (1:5000) for 1 hr. An enhanced chemiluminescence (ECL) system (Amersham Biosciences; GE Healthcare) was used for activation according to the manufacturer's guidelines. The film was then exposed for 3 s and developed on a Xograph Compact X5 film processor. The membrane was then stripped for incubation with rabbit anti-tubulin (1:5000) as a loading control, and then re-exposed as above (5s).

Ca^{2+} imaging and connectivity analysis

Isolated islets were incubated (37°C, 95% O_2/5% CO_2) for 1 h in fluo2-AM (10 µM; Teflabs, Austin, USA) diluted in a HEPES-bicarbonate buffer solution (120 mM NaCl, 4.8 mM KCl, 1.25 mM NaH_2PO_4, 24 mM $NaHCO_3$, 2.5 mM $CaCl_2$, 1.2 mM $MgCl_2$, 10 mM HEPES and 3 mM D-glucose; all Sigma). Functional multicellular Ca^{2+} imaging was achieved using a Nipkow spinning disk head, allowing rapid scanning of islet areas for long periods of time with minimal phototoxicity. A solid-state laser (CrystaLaser) controlled by a laser-merge module (Spectral Applied Physics) provided wavelengths of 491 nm to excite fluo-2 (rate = 0.5Hz; exposure time = 600 ms). Emitted light was filtered at 525/50 nm, and images captured with a highly sensitive 16-bit, 512 × 512 pixel back-illuminated EM-CCD camera (ImageEM 9100-13; Hamamatsu). Volocity^{TM} software (PerkinElmer) provided the user interface. During recordings, islets were maintained at 35°C to 36°C and continuously irrigated with bicarbonate buffer aerated with 95% O_2/5% CO_2. Connectivity

analysis was performed as previously described (8,45).

Measurement of insulin secretion in vitro.

Insulin secretion was measured in batch incubations essentially as described (63). In brief, batches of 20 islets from βPax6 KO or control mice were subjected to glucose-stimulated insulin secretion assay one week after tamoxifen administration (*n*=3 animals/genotype). Islets were incubated for 30 min. sequentially in 3 mM then 17 mM glucose. Islets were then lysed in lysis buffer (50 mM Tris.Cl pH 8.0, 150 mM NaCl, 1% v/v IGEPAL-C130) and nuclei pelleted. Insulin content of secreted and total fractions was determined by HTRF assay and normalised to DNA content of the nuclear fraction, assayed using CyQuant fluorescent dye.

ATP/ADP imaging

Islets were infected with an adenovirus containing cDNA encoding the ATP sensor Perceval (41) for 48 h to measure intracellular ATP dynamics. Excitation of the fluorescent probe was achieved using a 491 nm laser (Spectral Applied Physics; rate = 0.2 Hz; exposure time 600 ms). Emitted light was filtered at 525/50 nm and images captured as for Ca^{2+} imaging.

Total internal reflectance of fluorescence (TIRF) analysis

Islets were infected with an adenovirus encoding NPY(neuropeptide Y)-venus as described (64). Islets were dissociated as described (65) and the liberated cells allowed to adhere to poly-L-lysine-treated sterile glass slides for 24 h post transfection. Cells were then incubated for 1 h in HEPES-bicarbonate buffer (see Ca^{2+} imaging analysis) containing 3mM glucose at 37 °C. Fixation was performed by incubating the slides for 1h at room temperature for at room temperature in PBS supplemented with 4% (v/v) paraformaldehyde.

Imaging was performed as described (66) using a Nikon Eclipse Ti microscope equipped with a 100x/1.49NA TIRF objective, a TIRF/FRAP iLas2 module o control laser angle (Roper Scientific), a Quad Band TIRF Filter Cube (TRF89902 – Chroma). NPY-venus, localised in insulin-secreting vesicles (67), was excited using a 488 nm laser line, and images were acquired with an ORCA-Flash 4.0 camera (Hamamatsu) and Metamorph software (Molecular Device) was used for data capture. Laser angle was selected for an imaged section thickness of 150 - 180 nm. Images were analysed on ImageJ using a home-made macro. The script of the macro is available upon request.

Statistical analysis

Statistical significance was assessed using Student's t-test. Two-way ANOVA (with Bonferroni or Sidak multiple comparison test) was used to examine the effect of multiple variables. Statistical analyses were performed using Graph Pad Prism 7.0, ImageJ and IgorPro. Values represented are the mean ± SD.

ACKNOWLEDGEMENTS

Funded by grants to G.A.R. from the Wellcome Trust (Senior Investigator Award WT098424AIA), Diabetes UK (Project BDA 11/0004210), the MRC (UK; Project GO401641; Programme MR/J0003042/1) and by a Royal Society Research Merit Award. D.J.H. was supported by Diabetes UK R.D. Lawrence (12/0004431), EFSD/Novo Nordisk Rising Star and Birmingham Fellowships, a Wellcome Trust Institutional Support Award, an ERC Starting Grant (OptoBETA; 715884) and an MRC Project Grant (MR/N00275X/1) with G.A.R. D.J.H and G.A.R. were supported by Imperial Confidence in Concept (ICiC) Grants.

AUTHOR CONTRIBUTIONS

R.K.M., M.SN-T, P.C., R.M.C., T.J.P., I.L. and R.C. performed all experimental work and wrote the manuscript. G.A.R. supervised the work and wrote the manuscript. D.J.H. co-supervised the work and edited the manuscript. G.A.R. is the guarantor of the manuscript

DUALITY OF INTERESTS

The authors have no duality of interest to declare

Reference List

1. Rutter, G. A., Pullen, T. J., Hodson, D. J., and Martinez-Sanchez, A. (2015) Pancreatic beta cell identity, glucose sensing and the control of insulin secretion *Biochem. J.* **466,** 202-218

2. Maechler, P. and Wollheim, C. B. (2001) Mitochondrial function in normal and diabetic beta-cells *Nature.* **414,** 807-812

3. Ashcroft, F. M. and Rorsman, P. (2013) K(ATP) channels and islet hormone secretion: new insights and controversies *Nat. Rev. Endocrinol.* **9,** 660-669

4. Rutter, G. A., Theler, J.-M., Murta, M., Wollheim, C. B., Pozzan, T., and Rizzuto, R. (1993) Stimulated Ca2+ influx raises mitochondrial free Ca2+ to supramicromolar levels in a pancreatic β-cell line: possible role in glucose and agonist-induced insulin secretion *J. Biol. Chem.* **268,** 22385-22390

5. Rorsman, P. and Renstrom, E. (2003) Insulin granule dynamics in pancreatic beta cells *Diabetologia.* **46,** 1029-1045

6. Meda, P., Atwater, I., Gonccalves, A., Bangham, A., Orci, L., and Rojas, E. (1984) The topography of electrical synchrony among beta-cells in the mouse islet of Langerhans *Q. J. Exp. Physiol.* **69,** 719-735

7. Benninger, R. K. and Piston, D. W. (2014) Cellular communication and heterogeneity in pancreatic islet insulin secretion dynamics *Trends Endocrinol. Metab.* **25,** 399-406

8. Hodson, D. J., Mitchell, R. K., Bellomo, E. A., Sun, G., Vinet, L., Meda, P., Li, D., Li, W. H., Bugliani, M., Marchetti, P., Bosco, D., Piemonti, L., Johnson, P., Hughes, S. J., and Rutter, G. A. (2013) Lipotoxicity disrupts incretin-regulated human beta cell connectivity *J. Clin. Invest.* **123,** 4182-4194

9. Lee, H. J. and Colby, K. A. (2013) A review of the clinical and genetic aspects of aniridia *Semin. Ophthalmol.* **28,** 306-312

10. Yasuda, T., Kajimoto, Y., Fujitani, Y., Watada, H., Yamamoto, S., Watarai, T., Umayahara, Y., Matsuhisa, M., Gorogawa, S., Kuwayama, Y., Tano, Y., Yamasaki, Y., and Hori, M. (2002) PAX6 mutation as a genetic factor common to aniridia and glucose intolerance *Diabetes.* **51,** 224-230

11. Gosmain, Y., Marthinet, E., Cheyssac, C., Guerardel, A., Mamin, A., Katz, L. S., Bouzakri, K., and Philippe, J. (2010) Pax6 controls the expression of critical genes involved in pancreatic {alpha} cell differentiation and function *J. Biol. Chem.* **285,** 33381-33393

12. Wen, J. H., Chen, Y. Y., Song, S. J., Ding, J., Gao, Y., Hu, Q. K., Feng, R. P., Liu, Y. Z., Ren, G. C., Zhang, C. Y., Hong, T. P., Gao, X., and Li, L. S. (2009) Paired box 6 (PAX6) regulates glucose metabolism via proinsulin processing mediated by prohormone convertase 1/3 (PC1/3) *Diabetologia.* **52,** 504-513

13. Ahlqvist, E., Turrini, F., Lang, S. T., Taneera, J., Zhou, Y., Almgren, P., Hansson, O., Isomaa, B., Tuomi, T., Eriksson, K., Eriksson, J. G., Lyssenko, V., and Groop, L. (2012) A common variant upstream of the PAX6 gene influences islet function in man *Diabetologia.* **55,** 94-104

14. Sander, M., Neubuser, A., Kalamaras, J., Ee, H. C., Martin, G. R., and German, M. S. (1997) Genetic analysis reveals that PAX6 is required for normal transcription of pancreatic hormone genes and islet development *Gene Develop.* **11,** 1662-1673

15. Ashery-Padan, R., Zhou, X., Marquardt, T., Herrera, P., Toube, L., Berry, A., and Gruss, P. (2004) Conditional inactivation of Pax6 in the pancreas causes early onset of diabetes *Dev. Biol.* **269,** 479-488

16. Chen, Y., Feng, R., Wang, H., Wei, R., Yang, J., Wang, L., Wang, H., Zhang, L., Hong, T. P., and Wen, J. (2014) High-fat diet induces early-onset diabetes in heterozygous Pax6 mutant mice *Diabetes Metab Res. Rev.* **30,** 467-475

17. Parton, L. E., McMillen, P. J., Shen, Y., Docherty, E., Sharpe, E., Diraison, F., Briscoe, C. P., and Rutter, G. A. (2006) Limited role for SREBP-1c in defective glucose-induced insulin secretion from Zucker Diabetic Fatty rat islets: a functional and gene profiling analysis *Am J Physiol Endocrinol Metab.* **291,** E982-E994

18. Hart, A. W., Mella, S., Mendrychowski, J., van, H., V, and Kleinjan, D. A. (2013) The developmental regulator Pax6 is essential for maintenance of islet cell function in the adult mouse pancreas *PLoS. ONE.* **8,** e54173

19. Ahmad, Z., Rafeeq, M., Collombat, P., and Mansouri, A. (2015) Pax6 Inactivation in the Adult Pancreas Reveals Ghrelin as Endocrine Cell Maturation Marker *PLoS. ONE.* **10,** e0144597

20. Gosmain, Y., Katz, L. S., Masson, M. H., Cheyssac, C., Poisson, C., and Philippe, J. (2012) Pax6 is crucial for beta-cell function, insulin biosynthesis, and glucose-induced insulin secretion *Mol Endocrinol.* **26,** 696-709

21. Rutter, G. A. and Hodson, D. J. (2014) Beta cell connectivity in pancreatic islets: a type 2 diabetes target? *Cell Mol. Life Sci.* **72,** 453-467

22. Wicksteed, B., Brissova, M., Yan, W., Opland, D. M., Plank, J. L., Reinert, R. B., Dickson, L. M., Tamarina, N. A., Philipson, L. H., Shostak, A., Bernal-Mizrachi, E., Elghazi, L., Roe, M. W., Labosky, P. A., Myers, M. M., Jr. et al (2010) Conditional gene targeting in mouse pancreatic {beta}-cells: Analysis of ectopic Cre transgene expression in the brain *Diabetes.* **59,** 3090-3098

23. Gu, G., Dubauskaite, J., and Melton, D. A. (2002) Direct evidence for the pancreatic lineage: NGN3+ cells are islet progenitors and are distinct from duct progenitors *Development.* **129,** 2447-2457

24. Zhang, H., Fujitani, Y., Wright, C. V., and Gannon, M. (2005) Efficient recombination in pancreatic islets by a tamoxifen-inducible Cre-recombinase *Genesis.* **42,** 210-217

25. Pullen, T. J. and Rutter, G. A. (2013) When less is more: the forbidden fruits of gene repression in the adult beta-cell *Diabetes Obes. Metab.* **15,** 503-512

26. Thorrez, L., Laudadio, I., Van, D. K., Quintens, R., Hendrickx, N., Granvik, M., Lemaire, K., Schraenen, A., Van, L. L., Lehnert, S., guayo-Mazzucato, C., Cheng-Xue, R., Gilon, P., Van, M., I, Bonner-Weir, S. et al (2011) Tissue-specific disallowance of housekeeping genes: the other face of cell differentiation *Genome Res.* **21,** 95-105

27. Marselli, L., Thorne, J., Dahiya, S., Sgroi, D. C., Sharma, A., Bonner-Weir, S., Marchetti, P., and Weir, G. C. (2010) Gene expression profiles of Beta-cell enriched tissue obtained by laser capture microdissection from subjects with type 2 diabetes *PLoS. ONE.* **5,** e11499

28. Fadista, J., Vikman, P., Laakso, E. O., Mollet, I. G., Esguerra, J. L., Taneera, J., Storm, P., Osmark, P., Ladenvall, C., Prasad, R. B., Hansson, K. B., Finotello, F., Uvebrant, K., Ofori, J. K., Di, C. B. et al (2014) Global genomic and transcriptomic analysis of human pancreatic islets reveals novel genes influencing glucose metabolism *Proc. Natl. Acad. Sci. U. S. A.* **111,** 13924-13929

29. Elayat, A. A., el-Naggar, M. M., and Tahir, M. (1995) An immunocytochemical and morphometric study of the rat pancreatic islets *J. Anat.* **186,** 629-637

30. Katsuta, H., Aguayo-Mazzucato, C., Katsuta, R., Akashi, T., Hollister-Lock, J., Sharma, A. J., Bonner-Weir, S., and Weir, G. C. (2012) Subpopulations of GFP-Marked Mouse Pancreatic beta-Cells Differ in Size, Granularity, and Insulin Secretion *Endocrinology.*

31. Martinez-Sanchez, A., Nguyen-Tu, M. S., and Rutter, G. A. (2015) DICER Inactivation Identifies Pancreatic beta-Cell "Disallowed" Genes Targeted by MicroRNAs *Mol Endocrinol.* **29,** 1067-1079

32. Brun, P. J., Grijalva, A., Rausch, R., Watson, E., Yuen, J. J., Das, B. C., Shudo, K., Kagechika, H., Leibel, R. L., and Blaner, W. S. (2015) Retinoic acid receptor signaling is required to maintain glucose-stimulated insulin secretion and beta-cell mass *FASEB J.* **29,** 671-683

33. Sekine, N., Cirulli, V., Regazzi, R., Brown, L. J., Gine, E., Tamarit-Rodriguez, J., Girotti, M., Marie, S., MacDonald, M. J., Wollheim, C. B., and Rutter, G. A. (1994) Low lactate dehydrogenase and high mitochondrial glycerol phosphate dehydrogease in pancreatic β-cell. Potential role in nutrient sensing *J. Biol. Chem.* **269,** 4895-4902

34. Piccand, J., Strasser, P., Hodson, D. J., Meunier, A., Ye, T., Keime, C., Birling, M.-C., Rutter, G. A., and Gradwohl, G. (2014) Rfx6 maintains the functional identity of adult pancreatic β-cells *Cell Reports* **9,** 2219-2232

35. Dominguez-Gutierrez, G., Bender, A. S., Cirulli, V., Mastracci, T. L., Kelly, S. M., Tsirigos, A., Kaestner, K. H., and Sussel, L. (2017) Pancreatic beta cell identity requires continual repression of non-beta cell programs *J. Clin. Invest.* **127,** 244-259

36. Araki, K. and Inaba, K. (2012) Structure, mechanism, and evolution of Ero1 family enzymes *Antioxid. Redox. Signal.* **16,** 790-799

37. O'Brien, R. M. (2013) Moving on from GWAS: functional studies on the G6PC2 gene implicated in the regulation of fasting blood glucose *Curr. Diab. Rep.* **13,** 768-777

38. Deftos, L. J. (1991) Chromogranin A: its role in endocrine function and as an endocrine and neuroendocrine tumor marker *Endocr. Rev.* **12,** 181-187

39. Berg, J., Hung, Y. P., and Yellen, G. (2009) A genetically encoded fluorescent reporter of ATP:ADP ratio *Nat. Methods.* **6,** 161-166

40. Tarasov, A. I., Griffiths, E. J., and Rutter, G. A. (2012) Regulation of ATP production by mitochondrial Ca(2+) *Cell Calcium.* **52,** 28-35

41. Tarasov, A. I., Ravier, M. A., Semplici, F., Bellomo, E. A., Pullen, T. J., Gilon, P., Sekler, I., Rizzuto, R., and Rutter, G. A. (2012) The mitochondrial Ca^{2+} uniporter MCU is essential for glucose-induced ATP increases in pancreatic â-cells *PLoS One* **7,** e39722

42. Hodson, D. J., Tarasov, A. I., Gimeno, B. S., Mitchell, R. K., Johnston, N. R., Haghollahi, S., Cane, M. C., Bugliani, M., Marchetti, P., Bosco, D., Johnson, P. R., Hughes, S. J., and Rutter, G. A. (2014) Incretin-modulated beta cell energetics in intact islets of Langerhans *Mol. Endocrinol.* **28,** 860-871

43. Diraison, F., Parton, L., Ferre, P., Foufelle, F., Briscoe, C. P., Leclerc, I., and Rutter, G. A. (2004) Over-expression of sterol-regulatory-element-binding protein-1c (SREBP1c) in rat pancreatic islets induces lipogenesis and decreases glucose-stimulated insulin release: modulation by 5-aminoimidazole-4-carboxamide ribonucleoside (AICAR) *Biochem. J.* **378,** 769-778

44. Hodson, D. J., Schaeffer, M., Romano, N., Fontanaud, P., Lafont, C., Birkenstock, J., Molino, F., Christian, H., Lockey, J., Carmignac, D., Fernandez-Fuente, M., Le, T. P., and Mollard, P. (2012) Existence of long-lasting experience-dependent plasticity in endocrine cell networks *Nat. Commun.* **3:605. doi: 10.1038/ncomms1612.,** 605

45. Hodson, D. J., Mitchell, R. K., Marselli, L., Pullen, T. J., Brias, S. G., Semplici, F., Everett, K. L., Cooper, D. M., Bugliani, M., Marchetti, P., Lavallard, V., Bosco, D., Piemonti, L., Johnson, P. R., Hughes, S. J. et al (2014) ADCY5 couples glucose to insulin secretion in human islets *Diabetes.* **63,** 3009-3021

46. Sun, G., Reynolds, R., Leclerc, I., and Rutter, G. A. (2010) RIP2-mediated LKB1 deletion causes axon degeneration in the spinal cord and hind-limb paralysis *Disease Models and Mechanisms* **4,** 193-202

47. Solomou, A., Meur, G., Bellomo, E., Hodson, D. J., Tomas, A., Migrenne, L. S., Philippe, E., Herrera, P., Magnan, C., and Rutter, G. A. (2015) The zinc transporter Slc30a8/ZnT8 is required in a subpopulation of pancreatic alpha cells for hypoglycemia-induced glucagon secretion *J. Biol. Chem.* **290,** 21432-21442

48. Jonas, J. C., Sharma, A., Hasenkamp, W., Ilkova, H., Patane, G., Laybutt, R., Bonner-Weir, S., and Weir, G. C. (1999) Chronic hyperglycemia triggers loss of pancreatic beta cell differentiation in an animal model of diabetes *J Biol. Chem* **274,** 14112-14121

49. Brereton, M. F., Iberl, M., Shimomura, K., Zhang, Q., Adriaenssens, A. E., Proks, P., Spiliotis, I. I., Dace, W., Mattis, K. K., Ramracheya, R., Gribble, F. M., Reimann, F., Clark, A., Rorsman, P., and Ashcroft, F. M. (2014) Reversible changes in pancreatic islet structure and function produced by elevated blood glucose *Nat. Commun.* **5:4639. doi: 10.1038/ncomms5639.,** 4639

50. Pullen, T. J., Sylow, L., Sun, G., Halestrap, A. P., Richter, E. A., and Rutter, G. A. (2012) Over-expression of Monocarboxylate Transporter-1 (*Slc16a1*) in the pancreatic â-cell leads to relative hyperinsulinism during exercise *Diabetes* **61,** 1719-1725

51. Smith, S. B., Qu, H. Q., Taleb, N., Kishimoto, N. Y., Scheel, D. W., Lu, Y., Patch, A. M., Grabs, R., Wang, J., Lynn, F. C., Miyatsuka, T., Mitchell, J., Seerke, R., Desir, J., Vanden Eijnden, S. et al (2010) Rfx6 directs islet formation and insulin production in mice and humans *Nature.* **463,** 775-780

52. Adriaenssens, A. E., Svendsen, B., Lam, B. Y., Yeo, G. S., Holst, J. J., Reimann, F., and Gribble, F. M. (2016) Transcriptomic profiling of pancreatic alpha, beta and delta cell populations identifies delta cells as a principal target for ghrelin in mouse islets *Diabetologia.* **59,** 2156-2165

53. Bergsten, P., Grapengiesser, E., Gylfe, E., Tengholm, A., and Hellman, B. (1994) Synchronous oscillations of cytoplasmic Ca2+ and insulin release in glucose-stimulated pancreatic islets *J. Biol. Chem.* **269,** 8749-8753

54. Li, J., Yu, Q., Ahooghalandari, P., Gribble, F. M., Reimann, F., Tengholm, A., and Gylfe, E. (2015) Submembrane ATP and Ca2+ kinetics in alpha-cells: unexpected signaling for glucagon secretion *FASEB J.* **29,** 3379-3388

55. Johnston, N. R., Mitchell, R. K., Haythorne, E., Pessoa, M. P., Semplici, F., Ferrer, J., Piemonti, L., Marchetti, P., Bugliani, M., Bosco, D., Berishvilli, E., Duncanson, P., Watkinson, M., Broichhagen, J., Trauner, D. et al (2016) Beta cell hubs dicate pancreatic islet responses to glucose *Cell Metabolism* **24,** 389-401

56. Henquin, J. C. (2009) Regulation of insulin secretion: a matter of phase control and amplitude modulation *Diabetologia.* **52,** 739-751

57. Swisa, A., Avrahami, D., Eden, N., Zhang, J., Feleke, E., Dahan, T., Cohen-Tayar, Y., Stolovich-Rain, M., Kaestner, K. H., Glaser, B., Ashery-Padan, R., and Dor, Y. (2017) PAX6 maintains beta cell identity by repressing genes of alternative islet cell types *J. Clin. Invest.* **127,** 230-243

58. Oropeza, D., Jouvet, N., Budry, L., Campbell, J. E., Bouyakdan, K., Lacombe, J., Perron, G., Bergeron, V., Neuman, J. C., Brar, H. K., Fenske, R. J., Meunier, C., Sczelecki, S., Kimple, M. E., Drucker, D. J. et al (2015) Phenotypic characterization of MIP-CreERT1Lphi mice with transgene-driven islet expression of human growth hormone *Diabetes.* **64,** 3798-3807

59. Simpson, T. I., Pratt, T., Mason, J. O., and Price, D. J. (2009) Normal ventral telencephalic expression of Pax6 is required for normal development of thalamocortical axons in embryonic mice *Neural Dev.* **4:19. doi: 10.1186/1749-8104-4-19.,** 19-4

60. Soedling, H., Hodson, D. J., Adrianssens, A. E., Gribble, F. M., Reimann, F., Trapp, S., and Rutter, G. A. (2015) Limited impact on glucose homeostasis of leptin receptor deletion from insulin- or proglucagon-expressing cells *Mol Metab.* **4,** 619-630

61. Kone, M., Pullen, T. J., Sun, G., Ibberson, M., Martinez-Sanchez, A., Sayers, S., Nguyen-Tu, M. S., Kantor, C., Swisa, A., Dor, Y., Gorman, T., Ferrer, J., Thorens, B., Reimann, F., Gribble, F. et al (2014) LKB1 and AMPK differentially regulate pancreatic beta-cell identity *FASEB J.* **28,** 4972-4985

62. Parrizas, M., Maestro, M. A., Boj, S. F., Paniagua, A., Casamitjana, R., Gomis, R., Rivera, F., and Ferrer, J. (2001) Hepatic nuclear factor 1-alpha directs nucleosomal hyperacetylation to its tissue-specific transcriptional targets *Mol Cell Biol.* **21,** 3234-3243

63. Mitchell, R. K., Hu, M., Chabosseau, P. L., Cane, M. C., Meur, G., Bellomo, E. A., Carzaniga, R., Collinson, L. M., Li, W. H., Hodson, D. J., and Rutter, G. A. (2016) Molecular Genetic Regulation of Slc30a8/ZnT8 Reveals a Positive Association With Glucose Tolerance *Mol Endocrinol.* **30,** 77-91

64. Loder, M. K., Tsuboi, T., and Rutter, G. A. (2013) Live-cell imaging of vesicle trafficking and divalent metal ions by total internal reflection fluorescence (TIRF) microscopy *Methods Mol Biol.* **950:13-26. doi: 10.1007/978-1-62703-137-0_2.,** 13-26

65. Ravier, M. A. and Rutter, G. A. (2010) Isolation and culture of mouse pancreatic islets for ex vivo imaging studies with trappable or recombinant fluorescent probes *Methods Mol. Biol.* **633,** 171-184

66. Carrat, G. R., Hu, M., Nguyen-Tu, M. S., Chabosseau, P., Gaulton, K. J., van de Bunt, M., Siddiq, A., Falchi, M., Thurner, M., Canouil, M., Pattou, F., Leclerc, I., Pullen, T. J., Cane, M. C., Prabhala, P. et al (2017) Decreased STARD10 Expression Is Associated with Defective Insulin Secretion in Humans and Mice *Am. J. Hum Genet.* **100,** 238-256

67. Tsuboi, T. and Rutter, G. A. (2003) Multiple forms of kiss and run exocytosis revealed by evanescent wave microscopy *Curr. Biol.* **13,** 563-567

. **Figure Legends**

Figure 1: Inducible deletion of *Pax6* from pancreatic β cells does not affect β-cell mass

(A) Gene deletion was caused by tamoxifen-induced Pdx1CreER-mediated removal of exons 5, 5a and 6 of *Pax6*. (B) qRT-PCR (**p<0.01; Student's t-test; *n*=5 each genotype. Values represent mean ± SD) and (C) Western (immuno-) blot analysis of islets isolated from *βPax6*KO (*Cre*$^+$) and litter mate controls (*Cre*-) mice. Note the presence of a lower molecular mass band in the Cre$^+$ case reflecting the likely generation of a truncated Pax6 protein lacking exons 5 and 6. (D-F) Immunocytochemical analysis was performed as given under Experimental procedures. Pancreatic slices from wild-type controls (a-d) and PAX6 knockout mice (e-h) were stained for PAX6 (1:70), insulin (1:200) and glucagon (1:500) (scale bar = 50 μm). Images show staining of PAX6 (a, e), glucagon (b, f) and insulin (c, g). All channels were overlaid into a composite image with Dapi staining to visualise nuclear staining (d, h). (i) Percentage of PAX6-positive nuclei was significantly decreased in βPax6KO in whole islet cell populations compared to and litter mate controls. (****p<0.0001; Student's t-test; n=4 each genotype). (j) Percentage of PAX6 positive nuclei in beta was significantly decreased in βPax6KO mice. (****p<0.0001; Student's t-test; *n*=5 each genotype). A significant but smaller reduction in PAX6 positive nuclei was present in α cells. Values represent mean ± SD. β-cell mass and α-cell mass represent the percentage of respectively insulin- (G) and glucagon- (H) positive staining area over the total pancreas section using ImageJ software. β to α cell ratio (I) was obtained by measuring the total insulin/glucagon-positive area on each pancreas section. A total of five pancreas sections, evenly separated by 25 μm, from each animal and genotype were used (*n*=4 animals in each group; p=ns by Student's t test). Scale bar in D, 50 μm.

Figure 2: Deletion of *Pax6* in the β cell causes severe hyperglycaemia and reduces insulin levels.

(A) Fed glycaemic profile and (B) accompanying body weight of β*Pax6KO* and littermate control mice (n=2 *Cre*$^-$ and 4 *Cre*$^+$ mice). (C) Challenging mice with a 0.75 U/Kg body weight insulin injection showed normal insulin sensitivity, despite severe hyperglycaemia (*p<0.05, ****p<0.0001, two-way ANOVA; n=6 animals each genotype). Upon termination 2 weeks post tamoxifen treatment (D), glucose levels were increased (****p<0.0001; Student's t-test; n=7 *Cre*$^-$ and 6 *Cre*$^+$ mice) coupled with (E) decreased insulin levels (*p<0.05; Student's t-test; *n*=4 *Cre*$^-$ and 3 *Cre*$^+$ mice). (F) Five islets were lysed in acidified ethanol and insulin content determined by HTRF assay (*p<0.05; Student's t-test; *n*=14 *Cre*$^-$ and 12 *Cre*$^+$ replicates). (G). Insulin secretion

from isolated islets (see Experimental for details). **p<0.05 by Student's t-test for the effect of Pax6 deletion. (H) TIRF analysis of granule distribution involving *n*=30 separate cells for control, *n*=26 for null mouse islets. (I) Analysis of data obtained as in (H). Values represent mean ± SD.

Figure 3: Islet gene expression is altered by *Pax6* deletion.

RNA was extracted from islets isolated from *βPax6*KO and littermate control mice, reverse transcribed before assessment of gene expression. Expression of *Ins2* (A; **p<0.01), *Slc30a8* (B; *p<0.05), *Mafa* (C; ****p<0.0001), *Slc2a2* (D, ***p<0.001), *Glp1r* (E; *p<0.05), *Gck* (F, ns), *Slc16a1* (G, *p<0.05), *Ldha* (H, ns), *Gjd2* (I, ns), *Gcg* (J, ns) and *Ghrl* (K, *p<0.05; all paired Student's t-test *vs. Cre*$^-$; *n*=3-4 each genotype) was assessed in both β*Pax6*KO and littermate control mice. Values represent mean ± SD. (L) GSEA for disallowed genes (see Results). (M, N) Genes with increased (green) or decreased (red) expression in *βPax6*KO *versus* control mice, based on RNAseq analysis.

Figure 4: β*Pax6*KO islets exhibit reduced insulin positive cells but retain neuroendocrine properties.

(A) Pancreatic slices were stained for chromogranin A (1:200), insulin (1:200) and glucagon (1:1000) (scale bar = 50 μm). (B) Quantification of islet insulin:chromogranin A ratio (p<0.001; Student's t-test; n=50 *Cre*$^-$ and 75 *Cre*$^+$ islets). (C) as for (B), but glucagon:chromogranin A ratio (ns; Student's t-test; *n*=37 *Cre*$^-$ and 70 *Cre*$^+$ islets). Values represent mean ± SD.

Figure 5: Islets isolated from β*Pax6*KO mice display altered glucose-evoked ATP responses.

ATP rises in response to 11 mM glucose (A, representative traces) were reduced in *βPax6*KO islets (B; p<0.05; Student's t-test; *n*=9 *Cre*$^-$ and 13 *Cre*$^+$ islets). The number of cells that responded to 11 mM glucose was also substantially reduced (C&D; p<0.001; Student's t-test; *n*=9 *Cre*$^-$ and 13 *Cre*$^+$ islets). Similar findings were made using 8 mM glucose (E,F; p<0.001; Student's t-test; *n*=25 *Cre*$^-$ and 25 *Cre*$^+$ islets). Values represent mean ± SD.

Figure 6: β*Pax6KO* islets exhibit altered Ca^{2+} dynamics.

Nipkow spinning disk microscopy and the Ca^{2+} dye fluo2 were used to assess $[Ca^{2+}]_i$ dynamics in response to 11 mM glucose (A; p<0.001; Student's t-test; *n*=15 *Cre*$^-$ and 17 *Cre*$^+$ islets) or to 8 mM glucose (B; <0.001; Student's t-test; *n*=13 *Cre*$^-$ and 13 *Cre*$^+$ islets). No differences were apparent in the response to depolarisation with KCl (C; ns; Student's t-test; *n*=9 *Cre*$^-$ and 13 *Cre*$^+$ islets). Values represent mean ± SD.

Figure 7: Islet cell Ca^{2+} responses remain highly coordinated in β*Pax6KO* islets.

(A) Individual cellular Ca^{2+} responses from control (upper) and β*Pax6KO* (lower) islets. (B) Percentage of glucose-responsive islet cells (ns; Student's t-test; *n*= 15 *Cre*$^-$ and 17 *Cre*$^+$ islets). Connectivity analysis of glucose-stimulated Ca^{2+} traces revealed increases in both the percentage of correlated islet cell pairs (C; p=0.06) and correlative strength (D&E; *p<0.05; both Student's t-test; *n*=15 *Cre*$^-$ and 17 *Cre*$^+$ islets). Values represent mean ± SD.

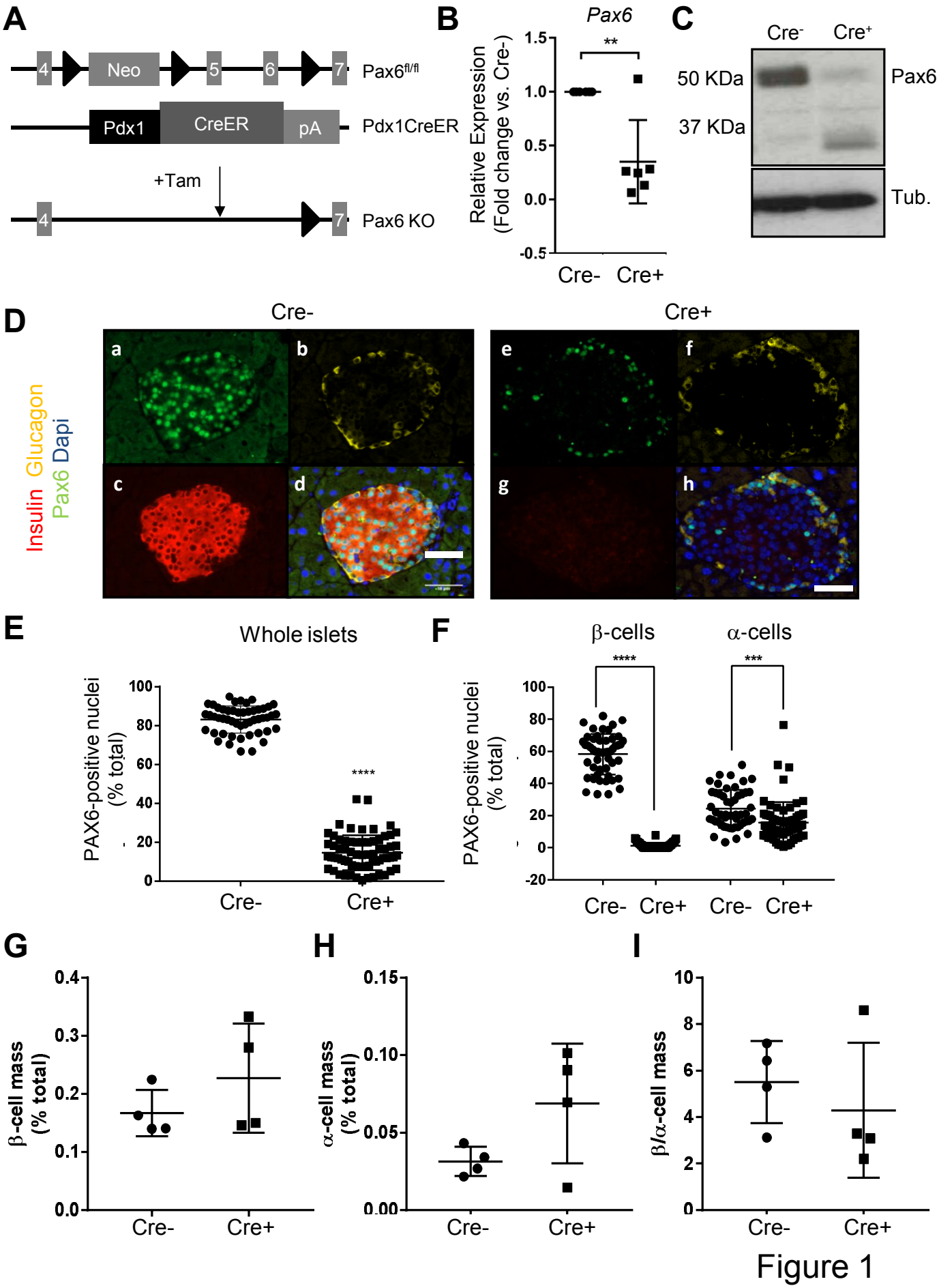
A
4
Neo
5
6
7
Pax6fl/fl
Pdx1
CreER
pA
Pdx1CreER
+Tam
4
7
Pax6 KO
B
Pax6
**
Relative Expression
(Fold change vs. Cre-)
1.5
1.0
0.5
0.0
-0.5
Cre-
Cre+
C
Cre-
Cre+
50 KDa
37 KDa
Pax6
Tub.
D
Cre-
Cre+
Insulin Glucagon
Pax6 Dapi
a
b
c
d
e
f
g
h
E
Whole islets
PAX6-positive nuclei
(% total)
100
80
60
40
20
0
****
Cre-
Cre+
F
β-cells
α-cells
****
***
PAX6-positive nuclei
(% total)
100
80
60
40
20
0
-20
Cre-
Cre+
Cre-
Cre+
G
β-cell mass
(% total)
0.4
0.3
0.2
0.1
0.0
Cre-
Cre+
H
α-cell mass
(% total)
0.15
0.10
0.05
0.00
Cre-
Cre+
I
β/α-cell mass
10
8
6
4
2
0
Cre-
Cre+

Figure 1

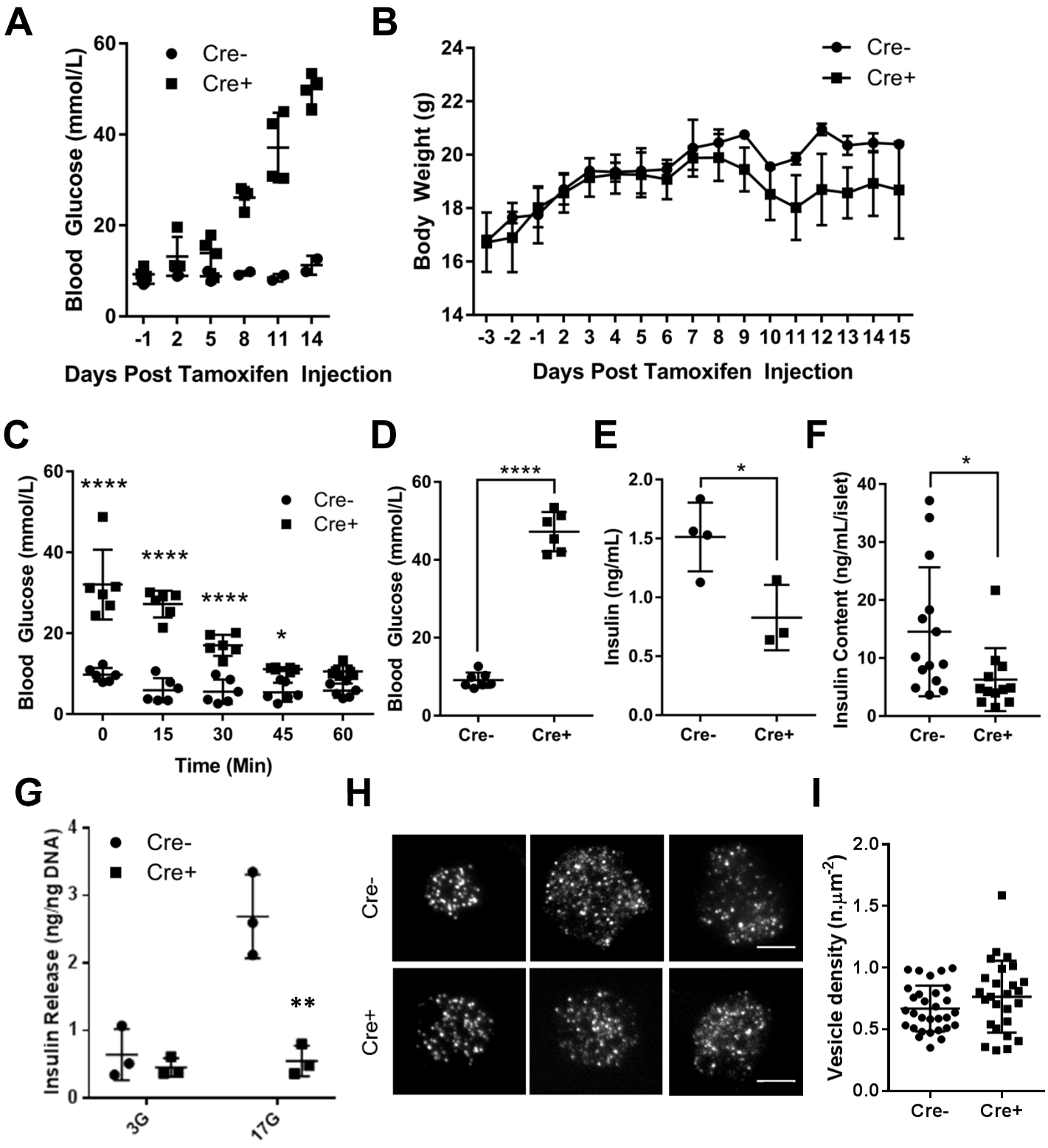
A
Blood Glucose (mmol/L)
Cre-
Cre+
Days Post Tamoxifen Injection
B
Body Weight (g)
Cre-
Cre+
Days Post Tamoxifen Injection
C
Blood Glucose (mmol/L)
Cre-
Cre+
Time (Min)
D
Blood Glucose (mmol/L)
E
Insulin (ng/mL)
F
Insulin Content (ng/mL/islet)
G
Insulin Release (ng/ng DNA)
Cre-
Cre+
3G
17G
H
Cre-
Cre+
I
Vesicle density (n.µm-2)

Figure 2

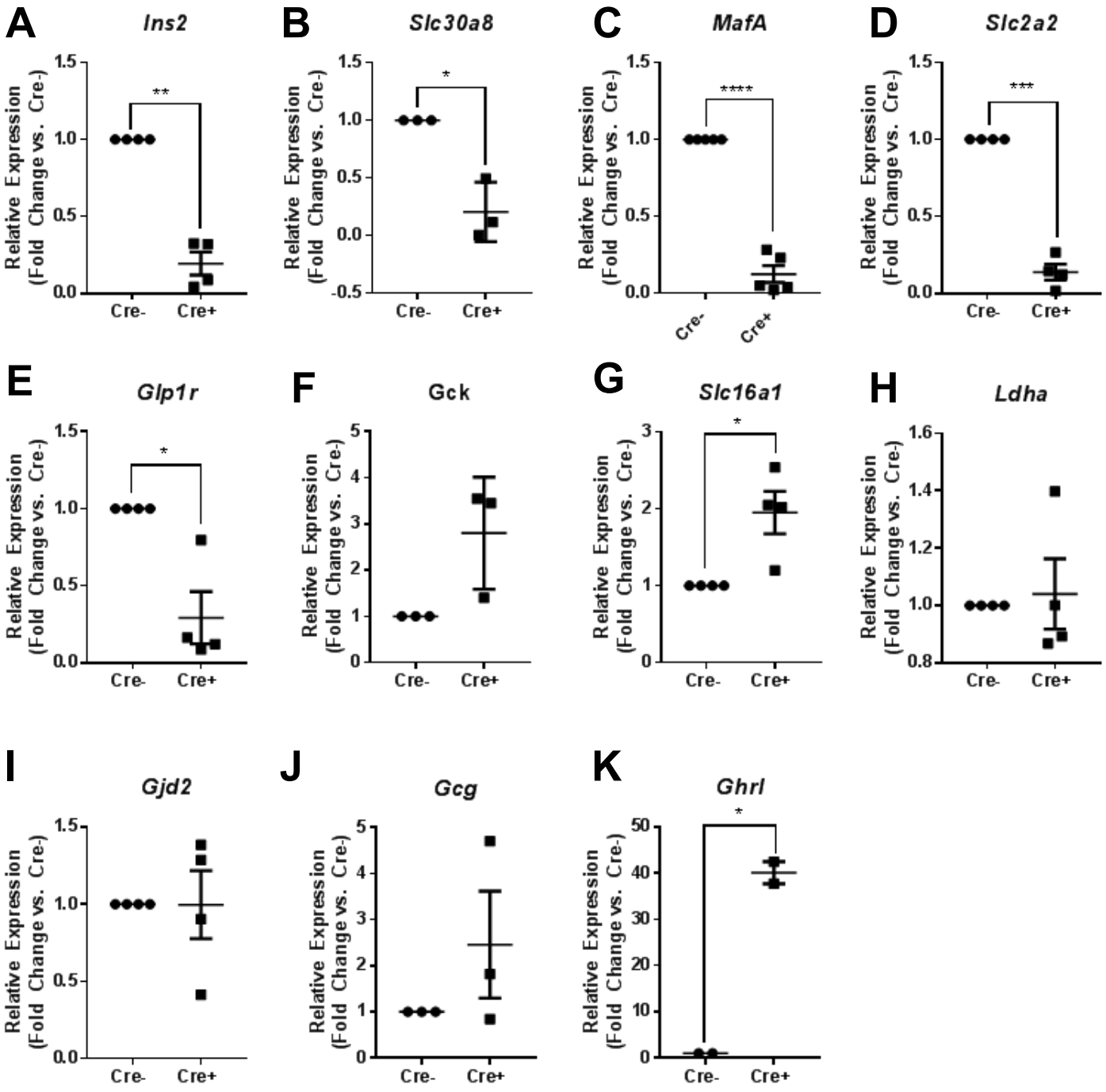
A
Ins2
B
Slc30a8
C
MafA
D
Slc2a2
E
Glp1r
F
Gck
G
Slc16a1
H
Ldha
I
Gjd2
J
Gcg
K
Ghrl
Relative Expression (Fold Change vs. Cre-)
Cre-
Cre+

Figure 3

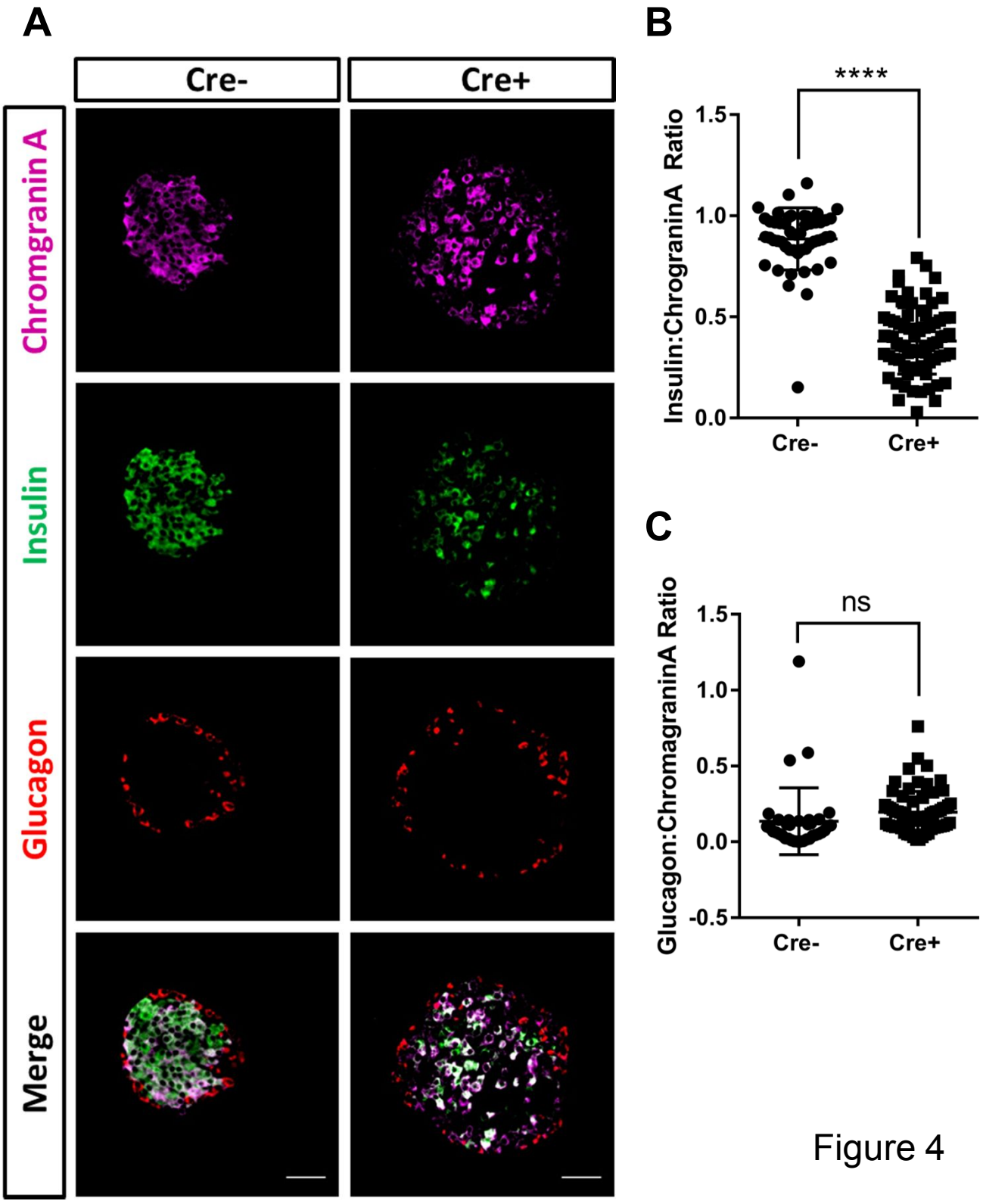
A
Cre-
Cre+
Chromgranin A
Insulin
Glucagon
Merge
B
****
Insulin:ChrograninA Ratio
1.5
1.0
0.5
0.0
Cre-
Cre+
C
ns
Glucagon:ChromagraninA Ratio
1.5
1.0
0.5
0.0
-0.5
Cre-
Cre+

Figure 4

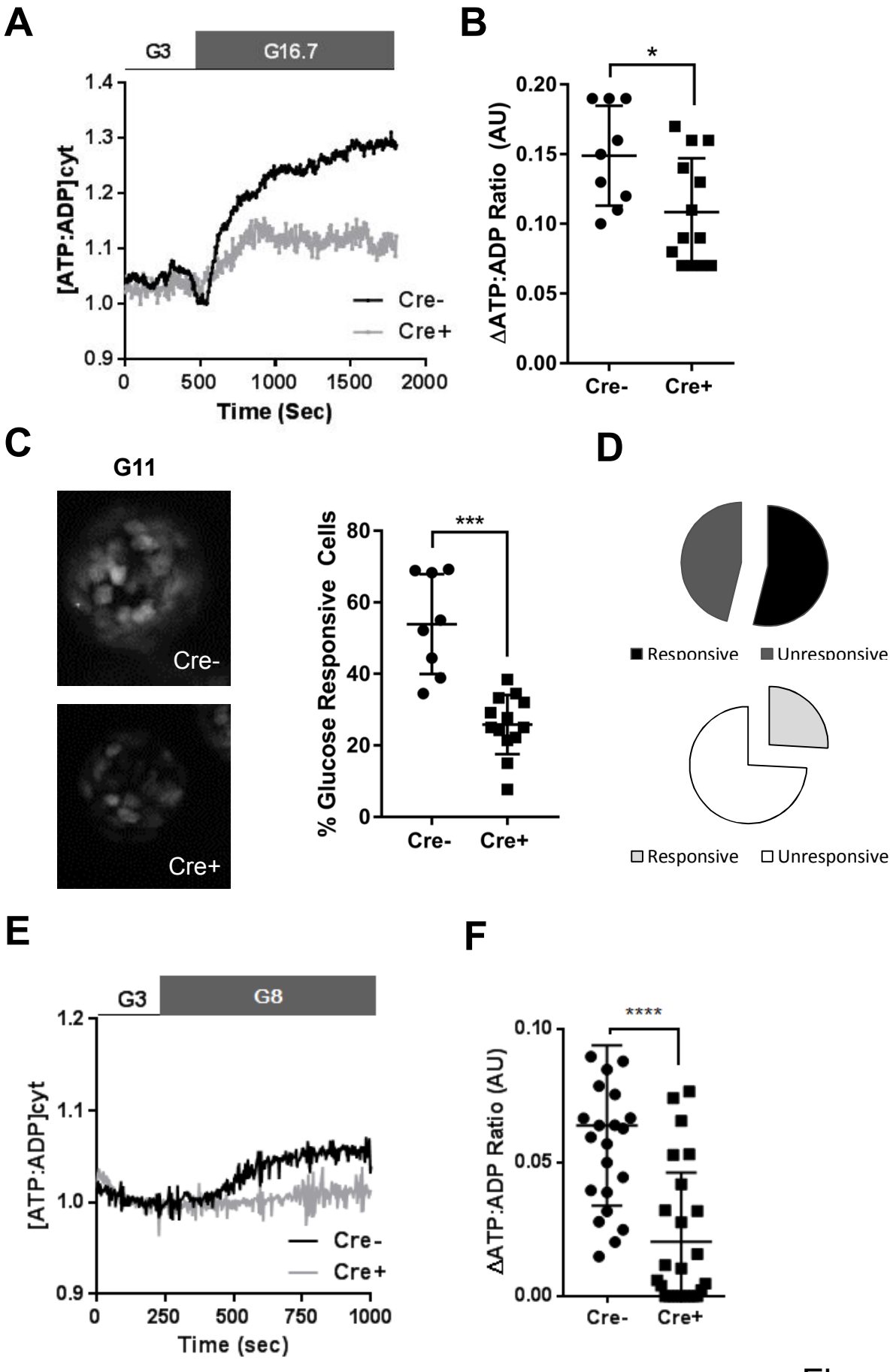
A
G3
G16.7
[ATP:ADP]cyt
Time (Sec)
Cre-
Cre+
B
ΔATP:ADP Ratio (AU)
*
Cre-
Cre+
C
G11
Cre-
Cre+
% Glucose Responsive Cells
***
D
Responsive
Unresponsive
E
G3
G8
[ATP:ADP]cyt
Time (sec)
F
ΔATP:ADP Ratio (AU)
****

Figure 5

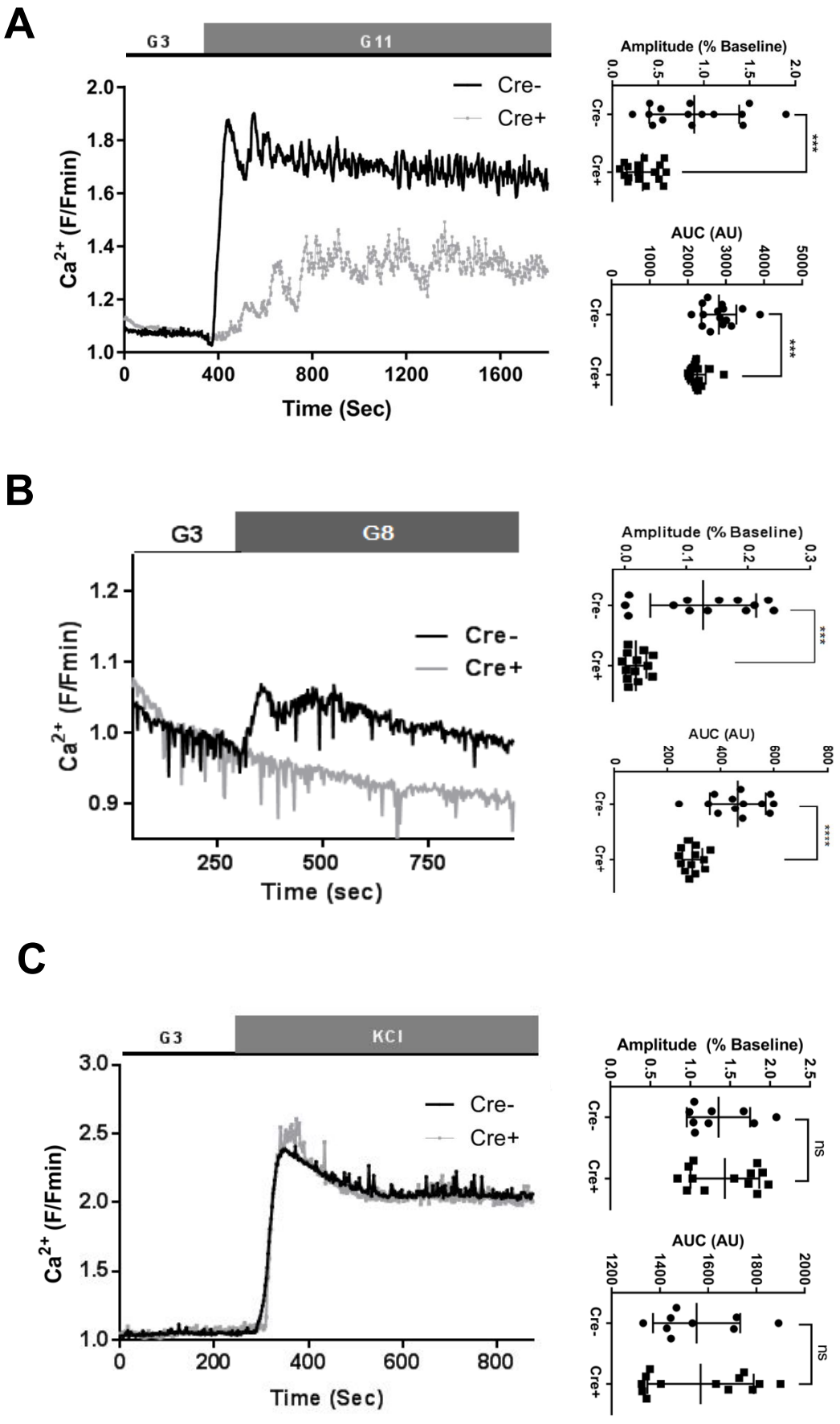
A
G3
G11
Cre-
Cre+
Ca2+ (F/Fmin)
Time (Sec)
Amplitude (% Baseline)
AUC (AU)
***
B
G3
G8
Time (sec)
****
C
KCl
ns

Figure 6

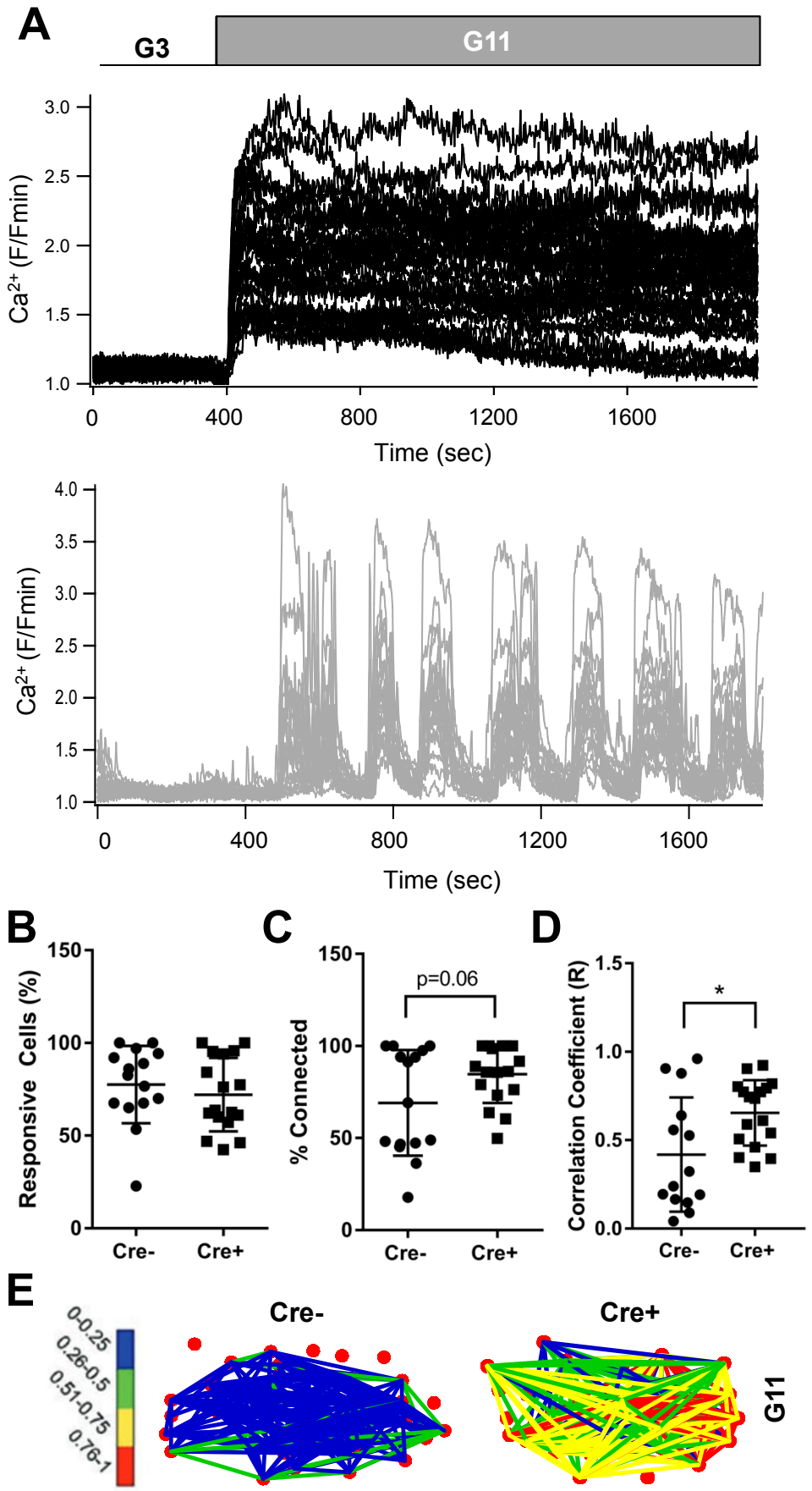
A
G3
G11
Ca2+ (F/Fmin)
Time (sec)
B
Responsive Cells (%)
Cre-
Cre+
C
% Connected
p=0.06
D
Correlation Coefficient (R)
*
E
0-0.25
0.26-0.5
0.51-0.75
0.76-1
G11

Figure 7